Pharmacological up-regulation of heart rate in ex vivo heart evaluation

Steen, Erik; Soltesz, Kristian; Li, Mei; Pigot, Henry; Paskevicius, Audrius; Liao, Qiuming; Steen, Stig

Published in:
Proceedings of the 10th IEEE Coinference on Control Technology and Applications (CCTA) 2026

DOI:
10.1109/CCTA62090.2026.11684254

2026

Document Version:
Peer reviewed version (aka post-print)

Pharmacological up-regulation of heart rate in *ex vivo* heart evaluation

Erik Steen[1] Kristian Soltesz[1] Mei Li[2] Henry Pigot[3] Audrius Paskevicius[4] Qiuming Liao[4] Stig Steen[4]

***Abstract*— In this paper, we present the development of a closed-loop drug delivery system for heart rate up-regulation in a novel *ex vivo* setup for functional evaluation of donor hearts. Such up-regulation is required to enable physiological testing aimed at supporting transplant decision-making. Clinical constraints prioritize safety over setpoint tracking performance. Accordingly, we develop a minimal dynamical model capturing the relevant response characteristics and use it to derive a closed-form upper bound on overshoot and tune a simple integrate-reset controller. We describe the real-time control system, which estimates heart rate from blood pressure measurements and regulates adrenaline infusion via a clinically certified pump. The controller design and modeling framework are discussed. Finally, the system is demonstrated in three *ex vivo* experiments on porcine hearts, showing closed-loop performance comparable to carefully executed manual drug titration. The controller is now used routinely in our ongoing evaluations.**

I. Introduction

A. Background

The increasing use of donation after circulatory death (DCD) has created a clinical demand for objective, repeatable assessment of donor heart function. In contrast to donation after brain death (DBD), DCD hearts experience a period of warm ischemia followed by reperfusion, and their functional recovery can vary substantially [1]. Whereas DBD donors retain intact circulation up to procurement, permitting in vivo functional assessment, DCD donors offer a substantially larger potential donor pool but cannot be assessed in vivo because circulation has ceased [2], [3], [4]. Without the possibility to assess organ function prior to implantation, "marginal" hearts from, for example, older donors are therefore excluded from contemporary transplantation programs, particularly DCD. As a consequence, only about one third of available donor hearts are utilized for transplantation [5].

The supply of donor hearts could be markedly increased if acceptance decisions were driven primarily by observed functional performance, excluding only those hearts that exhibit clinically relevant dysfunction. It is to this end the heart evaluation system (HES) is being developed, to evaluate the function of isolated hearts under circulatory load [6], [7]. The system delivers oxygenated perfusate—supplemented with pharmacological agents [8]—and allows the heart to pump as it would in the body. Afterload—the arterial flow impedance of the body—is emulated by a closed-loop controlled pneumatic system. Unlike simpler pre-clinical systems based on so-called Langendorff perfusion [9] or verbatim implementation of (active, but non-adaptive) Windkessel dynamics [10], this enables beat-to-beat response adaptation, making evaluation across clinically relevant workload cases possible. Figure 1 depicts the system during an ongoing evaluation of a porcine heart; Figure 2 provides a schematic drawing of the HES. This paper develops the dynamical model and control approach for heart rate regulation in the HES.

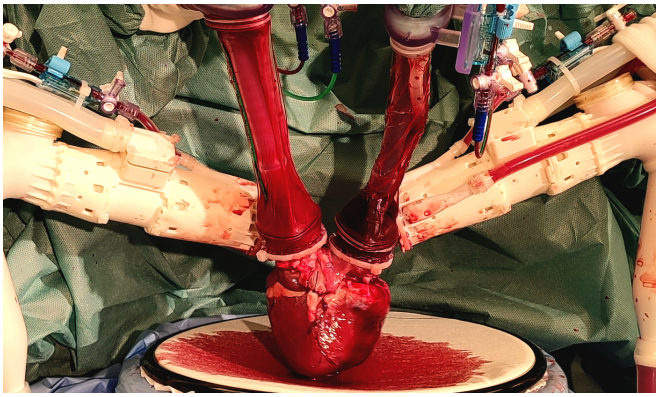

Fig. 1: Photo of a heart under evaluation.

B. Pharmacological up-regulation of heart rate

Rather than electrical pacing [11], we have aimed at pharmacological up-regulation of heart rate, to more closely resemble physiological conditions: the transplanted heart is denervated and relies on circulating catecholamines rather than autonomic neural input [12]. To do this, we have designed a computer-based control system that computes heart rate from available left ventricular pressure measurements read from the HES, and titrates dosing of adrenaline into the evaluation system perfusate using an infusion pump. We know from multiple porcine heart evaluation experiments that pharmacological support is needed to maintain a sufficiently high heart rate, and that drug sensitivity varies between and within subjects (as evident from the experimental results in section III). On multiple occasions we have also observed changes in heart rate that were not preceded by dosing changes. Hence it is clear that we are facing varying (uncertain) dynamics, in the presence of unknown disturbances.

*This work is part of a research program supported by the following foundations: Hans-Gabriel and Alice Trolle-Wachtmeister, Hjelm Family, Mats Paulsson, LMK, Knut and Alice Wallenberg via the Wallenberg AI, Autonomous Systems and Software Program (WASP). Authors with association 1 are members of the ELLIIT Strategic Research Area.

[1]Department of Automatic Control, Lund University, Lund, Sweden `erik.steen@control.lth.se`

[2]Department of Anesthesiology and Intensive Care, Skåne University Hospital and Lund University, Lund, Sweden

[3]Department of Translational Medicine, Artificial Intelligence and Bioinformatics in Cardiothoracic Sciences, Lund University, Lund, Sweden

[4]Department of Cardiothoracic Surgery, Skåne University Hospital and Lund University, Lund, Sweden

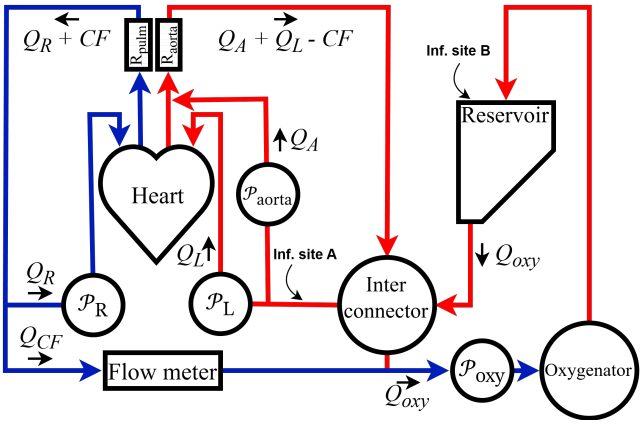

Fig. 2: Heart evaluation system (HES) flow schematic. Red: left (aortic) circuit; blue: right (pulmonary) circuit. Pumps $\mathcal{P}_L$, $\mathcal{P}_R$, and $\mathcal{P}_{\text{oxy}}$ drive flows Q_L, Q_R, and Q_{oxy} respectively; $\mathcal{P}_{\text{aorta}}$ provides retrograde aortic perfusion (Q_A) during startup. Adjustable afterloads R_{aorta} and R_{pulm} define arterial and pulmonary loading. Coronary return Q_{CF} enters a reservoir–oxygenator circuit via a flow meter. Infusion sites A and B indicate drug delivery points; site B was used in the three experiments.

The aim of the up-regulation is not to tightly track a heart rate setpoint. Instead, it is to maintain heart rate within a range suitable for functional evaluation, while avoiding large and prolonged overshoots caused by over-dosing. In the following we describe and demonstrate our approach to meet this aim.

II. Method

A. Heart evaluation system (HES)

The evaluation system [6] is shown in Figures 1 and 2. The heart is mounted with four cannulations—two venous inlets (left and right atria) and two arterial outlets (aorta and pulmonary artery)—enabling separate control of the aortic and pulmonary circuits. During startup, the aortic pump $\mathcal{P}_{\text{aorta}}$ provides retrograde aortic perfusion to establish coronary flow. When the heart is beating, the left pump $\mathcal{P}_L$ supplies perfusate to the left atrium via the left inlet. When perfusate is ejected from the left ventricle, one fraction perfuses the coronary circulation to sustain the myocardium, while the remaining fraction passes through the adjustable left afterload R_{aorta} and returns to the interconnector. Coronary venous return enters the right atrium, adding to the flow of the right pump $\mathcal{P}_R$, and is then pumped by the right ventricle to the pulmonary artery where it passes through the right afterload R_{pulm} and re-enters the right circuit.

Coronary flow transfers volume from the left side to the right side. The volume is continuously routed via a flow meter to the reservoir by way of the oxygenator circuit for reoxygenation and temperature control. The oxygenator pump $\mathcal{P}_{\text{oxy}}$ is operated at a higher flow than the coronary return so that perfusate is continuously drawn from the interconnector, ensuring stable oxygenation and heating throughout the perfusion circuit. A drug infusion line (e.g. adrenaline) was placed at infusion site B (reservoir), as shown in Figure 2.

B. Heart rate response dynamics

There are multiple phenomena contributing to the dynamic behavior relating drug (adrenaline) infusion and heart rate. The fundamental pharmacokinetics (PK) consist of mixing and elimination of drug within the *ex vivo* perfusion circuit.

While it is plausible that the pharmacokinetics could be modeled using compartment models, similar to those employed when synthesizing closed-loop anesthesia control systems [13], doing so for control would typically require online drug-concentration measurements within the perfusion circuit. We collected extensive offline perfusate samples with the objective of identifying such models; however, the resulting adrenaline concentration measurements were not sufficiently reliable to reconstruct concentration time courses across experiments. We therefore do not pursue concentration-based PK identification in the present work. Instead, we focus on capturing the combined pharmacokinetic–pharmacodynamic (PKPD) behavior in a lumped input–output model, using drug infusion rate as input and resulting heart rate as output.

Across many porcine heart evaluation experiments with manual drug titration, we have observed substantial inter-subject variability in heart rate response. Several physiological and experimental factors are likely to contribute; however, the relevant covariates and their predictive value have not yet been systematically established in this setting. The observed dynamics are also influenced by operating conditions of the evaluation system and by concomitant drugs used to stabilize hemodynamics during ongoing experiments.

The above suggests that identifying high-fidelity mechanistic models with broadly transferable parameters can be challenging in practice. However, unless high bandwidth or very tight setpoint-tracking demands are imposed, the required model fidelity is substantially lower. In our case, the design specification is to keep heart rate close to a user-specified setpoint while avoiding large overshoots and limiting settling time following setpoint changes or episodes of process disturbances. To quantitatively investigate the trade-offs between tracking accuracy, overshoot magnitude, and settling time, we nevertheless require a dynamic model.

Here we set out to devise a minimal, physiologically sound, lumped-parameter model that captures the phenomenological behavior we have observed in manually dosed experiments:

- Following an *increase* in drug infusion rate, the heart rate settles at a higher value, with a fast time constant T_1, on the time scale of seconds to a few minutes.

- Following a *decrease* in drug infusion rate, the heart rate decreases to a lower value, with a slow time constant T_0, on the time scale of tens of minutes.

For reference, *in vivo* adrenaline is cleared with a half-life of only a few minutes [14]; the substantially longer T_0

observed in our experiments reflects the absence of biological clearance pathways in the *ex vivo* perfusion circuit.

To maintain a physically and physiologically reasonable model, we consider the average drug concentration $q(t)$ [$\mu\mathrm{g\,L^{-1}}$]. The simplest possible (PK) model that links drug (adrenaline) infusion rate $u(t)$ [$\mu\mathrm{g\,min^{-1}}$] to $q(t)$ is

$$\dot{q}(t) = -\frac{1}{T_0}q(t) + \frac{1}{V}u(t), \tag{1}$$

where T_0 [min] is the time constant at which drug is eliminated from the perfusion circuit; V [L] is the circuit volume, and the time unit is chosen to be minutes, so that $\dot{q}(t)$ [$\mu\mathrm{g\,L^{-1}\,min^{-1}}$].

The simple (PD) model that can be used to model the settling dynamics following infusion rate increases is the following effect-site model,

$$\dot{q}_e(t) = \frac{1}{T_1}q(t) - \frac{1}{T_1}q_e(t), \tag{2}$$

where T_1 [min] is the settling time constant, and $q_e(t)$ is the effect-site concentration. In other words, the dynamics (2) linking $q(t)$ and $q_e(t)$ is a first-order system with transfer function

$$G_e(s) = \frac{1}{sT_1 + 1}. \tag{3}$$

The resulting heart rate could be expected to depend nonlinearly on an effect-site drug concentration $q_e(t)$. This could be modeled for example using a PD component comprising of a Hill sigmoid, to take into account saturation effects at low and high drug concentrations, as explained in e.g., [13]. However, a successful heart rate control system will operate close to a working point that is far from these saturations, and where the following linearization of the nonlinear PD model constitutes an adequate approximation (empirically tested in section III):

$$y(t) = y_0 + kq_e(t), \tag{4}$$

where $y(t)$ [$\mathrm{min^{-1}}$] is the modeled heart rate, y_0 [$\mathrm{min^{-1}}$] is a base-line heart rate in absence of drug, and k [$\mathrm{L\,\mu g^{-1}\,min^{-1}}$] is the linearization of the PD gain.

Introducing the state vector $\boldsymbol{x}(t) = [q(t)\ q_e(t)]^\top$, we arrive at the following state-space system description by combining (1), (2), and (4):

$$\begin{aligned}\dot{\boldsymbol{x}}(t) &= \underbrace{\begin{bmatrix} -\frac{1}{T_0} & 0 \\ \frac{1}{T_1} & -\frac{1}{T_1} \end{bmatrix}}_{A}\boldsymbol{x}(t) + \underbrace{\begin{bmatrix} \frac{1}{V} \\ 0 \end{bmatrix}}_{B}u(t), \\ y(t) &= y_0 + \underbrace{\begin{bmatrix} 0 & k \end{bmatrix}}_{C}\boldsymbol{x}(t).\end{aligned} \tag{5}$$

The model (5) captures the phenomenological behavior we are after, while being extremely simple. The volume V can be determined exactly, offline; T_0, T_1, and y_0 can be learnt (estimated) from data, as described below.

C. Controller design

Owing to the accumulative nature of the perfusion circuit, cf. (1), the dynamics are close to integrating. Thus, turning infusion off will result in a slow decay in y, rather than a rapid decline. With this observation in mind, we propose an extremely simple "integrate–reset" control law:

$$\begin{cases} \dot{u}(t) = \alpha, & r(t) > y(t), \\ u(t) = 0, & r(t) \le y(t), \end{cases} \tag{6}$$

with integration ramp speed α [$\mu\mathrm{g\,min^{-2}}$] as the only tunable parameter. The control law (6) can be written $u(t) = \alpha(t - t_0)$ where the assignment $t_0 \leftarrow t$ is performed whenever $r(t) \le y(t)$. The controller is initialized at $t = t_0$ to start at rest with $u_0 = u(t_0) = 0$. A larger value of α results in a faster response, but also a larger overshoot. For a given α, the overshoot magnitude is determined primarily by T_1, as $T_0 \gg T_1$.

Starting at $y(t_0) = y_0$ with $r > y_0$, the overshoot peak value $y_{\max}$ following the first control signal ramp resulting from (6) can be computed in two steps. Without loss of generality, we can assume $t_0 = 0$ to simplify our analysis. The first step is to determine the state $\boldsymbol{x}$ of (5) at the instance when $u(t)$ switches from $u(t) = \alpha(t - t_0) = \alpha t$ to $u(t) = 0$. This happens at time t_s at which $y(t_s) = r$. Using (5), starting in $\boldsymbol{x}(t) = \boldsymbol{0}$, with the ramp input $u(t) = \alpha t$, we can write down the analytic solution

$$\begin{aligned} y(t) = y_0 + \frac{\alpha k}{V}\Bigg[& T_0 t - T_0(T_0 + T_1) \\ & + \frac{T_0}{T_0 - T_1}\left(T_0^2 e^{-t/T_0} - T_1^2 e^{-t/T_1}\right)\Bigg]. \end{aligned} \tag{7}$$

Solving for $t = t_s$ (where $y(t_s) = r > y_0$) is only possible numerically as (7) lacks analytic solution. We therefore exploit our knowledge of $T_1 \ll T_0$, and treat the first state as an integrator, $\dot{x}_1(t) \approx \alpha t/V$, resulting in

$$y(t) \approx y_0 + \frac{\alpha k}{V}\left(\frac{t^2}{2} - T_1 t + T_1^2\left(1 - e^{-t/T_1}\right)\right). \tag{8}$$

While simpler, (8) still lacks analytic solution for $t = t_s$ with $y(t_s) = r > y_0$. However, we can see from (5) that the overshoot will be larger the larger t_s is, which is another way to say that the overshoot is increasing in $r - y_0$. Asserting $t_s \gg T_1$ we can then use (8) to produce the approximation

$$t_s \approx T_1 + \sqrt{\frac{2V}{\alpha k}(r - y_0) - T_1^2}. \tag{9}$$

The assumption $t_s \gg T_1$ implies that the fast filter (3) has had sufficient time to track the slower upstream state, such that $x_2(t) \approx x_1(t) - T_1\dot{x}_1(t)$ during the ramp phase. At the switching instance $t = t_s$, the output satisfies $y(t_s) = y_0 + kx_2(t_s) = r$, while the upstream state is approximately

$$x_1(t_s) \approx \frac{\alpha}{2V}t_s^2. \tag{10}$$

After the control input is reset to zero at $t = t_s$, the dynamics are governed by the homogeneous system in (5). The second state continues to increase as long as $x_1(t) > x_2(t)$, and the overshoot peak occurs at the time instant $t_p > t_s$ for which

$$x_1(t_p) = x_2(t_p). \tag{11}$$

Under the valid assumption $T_0 \gg T_1$, the upstream state $x_1(t)$ varies negligibly during the short post-switch transient of duration $\mathcal{O}(T_1)$. The overshoot peak is therefore attained when $x_2(t)$ has relaxed to $x_1(t_s)$, yielding the approximation

$$y_{\max} \approx y_0 + k x_1(t_s). \tag{12}$$

Using (10) together with the approximation (9) for t_s, we obtain the explicit overshoot estimate

$$y_{\max} \approx r + \frac{\alpha k T_1}{V} \sqrt{\frac{2V}{\alpha k}(r - y_0) - T_1^2}, \tag{13}$$

valid for $T_0 \gg T_1$ and $t_s \gg T_1$.

The intuitive take-away here is that the overshoot $y_{\max} - r$ is, according to (13), monotonically increasing in both T_1 and $r - y_0$, within the validity region of the model, $t_s \gg T_1$. By choosing a low value for y_0, a high value for r, and a high value for T_1, we can thus use (13) to compute a conservative (low) value of α to not exceed a specified acceptable overshoot $y_{\max}$. Likewise, the overshoot increases as perfusate volume V decreases, and the overshoot increases in the PD gain parameter k. As a reminder, the bound (13) assumes $T_0 \gg T_1$ and $t_s \gg T_1$. Under these conditions, (13) over-estimates the actual overshoot, primarily because approximation (12) ignores the slow decay of x_1 during the post-switch transient $[t_s, t_p]$, and approximation (10) treats x_1 as a pure integrator during the ramp phase. This conservatism is verified numerically in Fig. 3.

Based on the above discussion, we have used $y_0 = 65\ \text{min}^{-1}$, which was the lowest observed heart rate in absence of pharmacological stimulation in our porcine ex vivo experiments; $r = 160\ \text{min}^{-1}$, which is the largest setpoint we anticipate using; $T_1 = 2$ min, which is slower than the response speed observed when previously giving manual bolus doses. Furthermore, the actual perfusate volume $V = 4$ L was used alongside the PD gain parameter estimate $k = 5\ \text{L}\,\mu\text{g}^{-1}\,\text{min}^{-1}$, gauged from previous bolus responses. It was decided that $y_{\max} - r = 25\ \text{min}^{-1}$ is an admissible overshoot. Altogether, this translates into employing the controller parameter tuning $\alpha = 2/3\ \mu\text{g}\,\text{min}^{-2}$.

Figure 3 shows a simulated response of the closed-loop control system that validates the overshoot approximation used for controller tuning. In this simulation, we have used $T_0 = 30$ min.

D. Heart rate detection and filtering

Left ventricular pressure was used to estimate heart rate via a prominence-based peak detector described in [15]. The exact peak locations are subject to timing jitter, even during steady beating. The intervals between subsequent maximal systolic-phase pressure gradients $dP(t)/dt$ are less prone to jitter and were therefore used to detect heart rate.

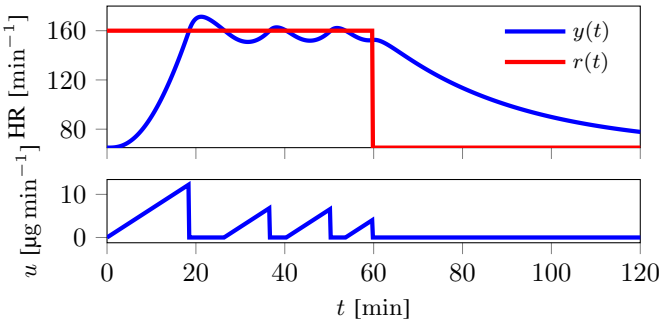

Fig. 3: Simulated response, verifying that the actual overshoot stays well below the $25\,\text{min}^{-1}$ bound stipulated by the over-estimation by (13). The simulation starts at $t = 0$ min with heart rate $y(0) = y_0 = 65\ \text{min}^{-1}$, at which time the closed-loop controller is activated with a setpoint of $r = 160\ \text{min}^{-1}$. At $t = 60$ min, the controller is effectively deactivated by setting $r = y_0$.

To avoid spurious controller resets caused by short arrhythmic episodes, the median value from a trailing window of width T_w [s] is used. (Matching at -3 dB (half-power) gain, this corresponds to a first-order low-pass filter with time constant $T_f \approx 0.36 T_w$.) The resulting heart rate, y, served as the controller input. In the first experiment, the average was taken over a window of length $T_w = 6$ s. This short window led to premature resets of the integrating control signal, increasing the time to reach the setpoint. In subsequent experiments, the median heart rate value was used instead over a lengthened trailing window of $T_w = 60$ s.

E. Real-time control system

Pressure was recorded using disposable pressure transducers (Meritrans DTXPlus®; Merit Medical, USA) connected to an Arduino-based data acquisition unit with sampling frequency 333 Hz. Adrenaline infusions were titrated via infusion site B, see Figure 2, by a syringe pump (Alaris® TIVA; CareFusion, USA) and for which we have written Python serial-over-USB drivers. The controller was implemented in Python, in a custom-designed threaded environment. Left ventricular pressure was streamed online from the data-acquisition unit and the resulting heart rate estimate was updated at 1 Hz. The filtered heart rate signal was then used to evaluate the integrate–reset law (6), and the commanded infusion rate was updated at 1 Hz. A graphical user interface was developed to monitor heart rate and infusions in real-time during experiments; all data was logged to file.

F. Experiments

The animals (Sus scrofa domesticus, body weight 49, 42, and 37 kg) were sedated and anaesthetized according to the protocol described in [6]. Animals were euthanized by exsanguination under deep anaesthesia at the time of cardiectomy.

When the heart was mounted in the HES and beating normally, the left and right pumps were set to achieve left

and right cardiac outputs of $45\,\mathrm{mL/min/kg}$ body weight (reference normal-stimulation value reported in [6]).

Experiments 1 and 2 followed a protocol comprising three sequential heart rate setpoints followed by a final decay phase. The setpoint was advanced to the next value once two controller resets had been observed.

During experiment 3, the heart rate setpoint was $100\,\mathrm{min}^{-1}$ while two left-heart evaluation maneuvers were performed to investigate control performance during hemodynamic tests representative of a heart evaluation experiment.

For these tests, noradrenaline was needed in addition to adrenaline, to provide both inotropic (contractile strength) and chronotropic (pacing) support. To this end, adrenaline was replaced by an evaluation drug mixture described further in [6]. The adrenaline-to-noradrenaline ratio in the infusion mixture was 1:1, and the adrenaline concentration (drug mass per infused volume) was kept equal to that used in experiments 1 and 2.

Two types of hemodynamic tests were used: one bringing the heart to a high-flow working point, and one bringing the heart to a high-pressure working point. For the former, afterload impedance was set to yield $AP \approx 100/70\,\mathrm{mmHg}$, and cardiac output was increased until $LAP = 10\,\mathrm{mmHg}$; the corresponding maximum cardiac output was recorded. For the latter, cardiac output was held at $70\,\mathrm{mL\,min^{-1}\,kg^{-1}}$ (reference high-stimulation value reported in [6]), and afterload impedance was increased (raising systolic and diastolic AP) until $LAP = 10\,\mathrm{mmHg}$; the maximum achieved arterial pressures were recorded.

All experiments were approved by the Ethics Committee for Animal Research at the University of Lund (approval No. 5.8.18-22454/2021) and conducted in accordance with Directive 2010/63/EU of the European Convention for the Protection of Vertebrate Animals Used for Experimental and Other Scientific Purposes.

III. Results

Figure 4 shows the measured heart rate together with fitted-model trajectories for the three experiments. Since the model (5) is a local linearization (4), we report both global fits (one parameter set per experiment, shown in red) and piecewise fits (separate parameter sets in two operating regions, shown in green); consistency of the latter within narrower windows tests the local-linearization premise.

For experiments 1–2, the split was placed immediately before the setpoint change from 120 to $160\,\mathrm{min}^{-1}$. For experiment 3, the split was placed before and after the evaluation maneuver (excluding minutes 37–63).

The parameters were estimated by minimizing the ℓ_2 norm of the prediction error between the measured heart rate and the output of (5), driven by the same control input u as applied in the experiment.

For our design, the estimates of T_0 and T_1 are the ones of highest interest. The global estimates for the three experiments were $T_0 = \{44, 18, 106\}\mathrm{min}$ and $T_1 = \{0.1, 5.2, 0.6\}\mathrm{min}$, confirming substantial variability. In contrast, the piecewise fits produced more consistent estimates of the slow time constant T_0 (part 1: $\{28, 10, 21\}\mathrm{min}$; part 2: $\{37, 12, 29\}\mathrm{min}$), supporting the interpretation that the model is locally adequate over narrower operating ranges. The fast time constant estimate T_1 was less consistent (part 1: $\{0.1, 6.6, 0.9\}\mathrm{min}$; part 2: $\{0.1, 6.0, 0.6\}\mathrm{min}$). Three subsequent experiments with operator-applied bolus, sawtooth, and step inputs yielded global $T_0 = \{38, 79, 75\}\mathrm{min}$ and $T_1 = \{14, 2.1, 0.1\}\mathrm{min}$, broadly consistent with the ranges above.

Experiment 1: The controller reached and maintained the first two heart rate setpoints but did not reach the third setpoint of $160\,\mathrm{min}^{-1}$. Brief fluctuations (noise) in the heart rate estimate intermittently triggered the controller and repeatedly reset the infusion rate before the setpoint was reached. To address this, the $6\,\mathrm{s}$ averaging window for heart rate calculation was exchanged for a $60\,\mathrm{s}$ median window, as described in section II-D.

Experiment 2: The controller reached the first two heart rate setpoints. Relative to Experiment 1, substantially higher infusion rates were required to reach the $140\,\mathrm{min}^{-1}$ setpoint (approximately twice the mean infusion rate). The heart rate also exhibited pronounced transient variability, most clearly around $140\,\mathrm{min}$ into the experiment (Figure 4). Given the pronounced heart rate variability and the high infusion rates required to reach $140\,\mathrm{min}^{-1}$ and maintain $120\,\mathrm{min}^{-1}$, the third setpoint ($160\,\mathrm{min}^{-1}$) was not attempted and the infusion was turned off to initiate the decay phase.

Experiment 3: The heart rate was initially $72\,\mathrm{min}^{-1}$, and reached the $100\,\mathrm{min}^{-1}$ setpoint after $\sim 7\,\mathrm{min}$. After an initial overshoot of $14\,\mathrm{min}^{-1}$, the heart rate remained within $\pm 3\,\mathrm{min}^{-1}$ of the setpoint. The heart produced a CO_L of $4.2\,\mathrm{L/min}$ during the high-flow test and the heart rate increased to $120\,\mathrm{min}^{-1}$. The high-pressure test reached $155/140\,\mathrm{mmHg}$ arterial pressure with a heart rate of $138\,\mathrm{min}^{-1}$.

Across the experiments, our simple controller managed to track the setpoint with a $4 \pm 4\ \mathrm{min}^{-1}$ (mean$\pm$std) error (rise and decay phases excluded).

IV. Discussion and Conclusion

This paper has described the development of a pharmacological control system for heart rate up-regulation in a novel *ex vivo* heart evaluation system. A dynamical model and controller with focus on simplicity in the presence of large response variability were developed, implemented, and evaluated in three porcine experiments. The result is a controller with only one tunable parameter constituting a trade-off between response speed and overshoot. Experiments 1 and 3 showed that the heart rate setpoint could be adequately tracked. In contrast, experiment 2 displayed atypical responsiveness: with approximately twice the mean infusion rate required to reach and sustain the first setpoint compared with Experiment 1. Such variability is expected across hearts and may be accentuated in injured preparations. Experiment 2 further highlights that variability can be both inter- and intra-subject: the heart rate shifted rapidly between regimes, on a timescale that could not be coupled to the

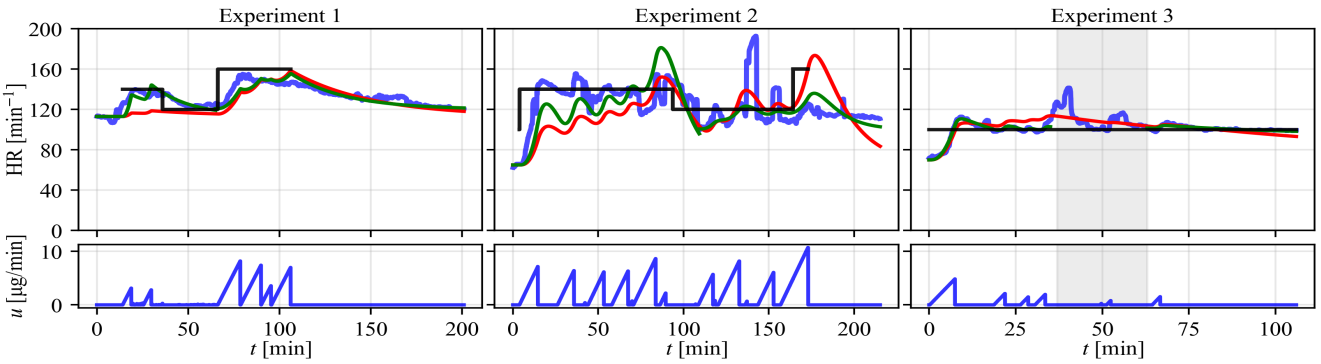

Fig. 4: Global and piecewise model fits for the three experiments. Upper row: measured heart rate $y(t)$ (blue), global fit (red), piecewise fit (green) and setpoint (black). Lower row: infusion rate $u(t)$. Experiment 3: the shaded region (37 min to 63 min) corresponds to the flow- and pressure tests described in section II-F; deviations from setpoint within this region are co-located with the tests.

infusion profile. A controller that escalates infusion until the setpoint is reached warrants operator oversight in its current form, particularly for marginal or injured hearts. Future iterations should incorporate explicit safety constraints and criteria for detecting weak or saturating responsiveness to prevent continued escalation when the expected effect is absent.

Experiment 3 highlighted that loading conditions can modulate heart rate, and thus act as a disturbance on the control system.

All-in-all, the results show that reliable heart rate regulation in an *ex vivo* setting can be achieved with very simple control. The integrate–reset structure provides predictable behavior with a single tuning parameter. Closed-loop performance matched careful manual titration, while reducing operator workload and improving repeatability. This makes the proposed system a practical and robust solution, now used routinely in our ongoing ex vivo evaluations, replacing manual titration.

References

[1] D. J. Hausenloy and D. M. Yellon, "Myocardial ischemia–reperfusion injury: A neglected therapeutic target," *Journal of Clinical Investigation*, vol. 123, no. 1, pp. 92–100, 2013. DOI: 10.1172/JCI62874.

[2] K. K. Dhital, A. Iyer, M. Connellan, et al., "Adult heart transplantation with distant procurement and ex-vivo preservation of donor hearts after circulatory death: A case series," *Lancet*, vol. 385, no. 9987, pp. 2585–2591, 2015. DOI: 10.1016/S0140-6736(15)60038-1.

[3] S. Messer, S. Rushton, L. Simmonds, et al., "A national pilot of donation after circulatory death (dcd) heart transplantation within the united kingdom," *Journal of Heart and Lung Transplantation*, vol. 42, no. 8, pp. 1120–1130, 2023. DOI: 10.1016/j.healun.2023.03.006.

[4] J. Louca, M. Öchsner, A. Shah, et al., "The international experience of in-situ recovery of the dcd heart: A multicentre retrospective observational study," *EClinicalMedicine*, vol. 58, p. 101 887, 2023. DOI: 10.1016/j.eclinm.2023.101887.

[5] J. Nilsson, V. Jernryd, G. Qin, et al., "A nonrandomized open-label phase 2 trial of nonischemic heart preservation for human heart transplantation," *Nature Communications*, vol. 11, p. 2976, 2020. DOI: 10.1038/s41467-020-16782-9.

[6] S. Steen, A. Paskevicius, Q. Liao, and E. Steen, "Ex vivo evaluation of the whole heart function allowing selective investigation of the right and left heart," *Scandinavian Cardiovascular Journal*, vol. 58, no. 1, p. 2418084, 2024. DOI: 10.1080/14017431.2024.2418084.

[7] H. Pigot, K. Soltesz, and S. Steen, "Ex vivo working porcine heart model," in *Experimental Models of Cardiovascular Diseases: Methods and Protocols*, ser. Methods in Molecular Biology, K. Ishikawa, Ed., vol. 2803, Humana Press, 2024, pp. 87–107. DOI: 10.1007/978-1-0716-3846-0_7.

[8] S. Steen, T. Sjöberg, Q. Liao, G. Bozovic, and B. Wohlfart, "Pharmacological normalization of circulation after acute brain death," *Acta Anaesthesiologica Scandinavica*, vol. 56, no. 8, pp. 1006–1012, 2012. DOI: 10.1111/j.1399-6576.2012.02721.x.

[9] R. M. Bell, M. M. Mocanu, and D. M. Yellon, "Retrograde heart perfusion: The langendorff technique of isolated heart perfusion," *Journal of Molecular and Cellular Cardiology*, vol. 50, no. 6, pp. 940–950, 2011. DOI: 10.1016/j.yjmcc.2011.02.017.

[10] B. Gellner et al., "The implementation of an adjustable afterload module for ex situ heart perfusion," *Cardiovascular Engineering and Technology*, vol. 11, no. 1, pp. 96–110, 2020. DOI: 10.1007/s13239-019-00447-w.

[11] D. S. Usai, E. Aasum, and M. B. Thomsen, "The isolated, perfused working heart preparation of the mouse – advantages and pitfalls," *Acta Physiologica (Oxf.)*, vol. 241, no. 4, e70023, 2025. DOI: 10.1111/apha.70023.

[12] F. M. Bengel, P. Ueberfuhr, N. Schiepel, S. G. Nekolla, B. Reichart, and M. Schwaiger, "Effect of sympathetic reinnervation on cardiac performance after heart transplantation," *New England Journal of Medicine*, vol. 345, no. 10, pp. 731–738, 2001. DOI: 10.1056/NEJMoa010519.

[13] K. Soltesz, K. van Heusden, and G. A. Dumont, "Models for control of intravenous anesthesia," in *Automated drug delivery in anesthesia*, D. Copot, Ed., Elsevier, 2020, pp. 119–166. DOI: 10.1016/B978-0-12-815975-0.00010-2.

[14] W. E. Clutter, D. M. Bier, S. D. Shah, and P. E. Cryer, "Epinephrine plasma metabolic clearance rates and physiologic thresholds for metabolic and hemodynamic actions in man," *Journal of Clinical Investigation*, vol. 66, no. 1, pp. 94–101, 1980. DOI: 10.1172/JCI109840.

[15] K. Soltesz, "Robust computation of pulse pressure variations," *Biomedical Signal Processing and Control*, vol. 39, pp. 197–203, 2018. DOI: 10.1016/j.bspc.2017.07.021.